URSI GASS 2023, Sapporo, Japan, 19 – 26 August 2023

Induction Motor High-Frequency Behavioral Modeling Using PINN

Zhenyu Zhao* and Kye Yak See
Nanyang Technological University, Singapore; e-mail: zhenyu.zhao@ntu.edu.sg; ekysee@ntu.edu.sg

Abstract

Induction motor high-frequency modeling is critical for evaluating motor terminal overvoltages and conducted electromagnetic interference (EMI) in motor drive systems. The paper presents a high-frequency behavioral modeling method of induction motors using physics informed neural network (PINN). Compared with existing methods, this method owes high precision, good generality, and easy parameterization. The case study validates its capability and effectiveness.

1 Introduction

Motor drive systems are widely used in many industrial applications. As shown in Figure 1, a motor drive system typically consists of an induction motor and a drive, interconnected by the cable. The impedance mismatch between the motor and the cable can cause overvoltage at the motor terminal [1]. In addition, the drive switching can cause conducted EMI [2], which can affect nearby sensitive electrical/electronic devices in various ways. Induction motor high-frequency modeling is critical to evaluate the overvoltage and the conducted EMI in motor drive systems [3].

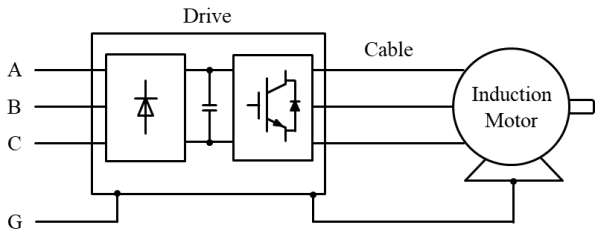

Figure 1. Diagram of a typical motor drive system.

There are two main categories of high-frequency modeling methods for induction motors, namely numerical modeling and behavioral modeling. Numerical modeling can be used to evaluate motor design decision's effects on motor performance before motor manufacturing [4]. However, in order to ensure the accuracy of the model, numerical modeling requires accurate motor internal structure and material information in advance. This is often difficult given the complex structure and composition inside the motor. In contrast, behavioral modeling does not require information about the motor's internal structure and materials, and is based on motor impedance measurements and curve-fitting. To date, behavioral modeling has been widely used to predict the overvoltage and the conducted EMI in motor drive systems [5]-[6].

This paper introduces a new induction motor high-frequency behavioral modeling method using PINN. The motor model comprises an improved form of the 3-phase equivalent circuit in reference [7]. The improved model includes more circuit elements to improve its accuracy. Besides, the circuit is modified to be symmetrical about its phase-start and phase-end, which makes it applicable to both Y and Δ connections without recomputing the model circuit element values when varying the motor connection (i.e., Y to Δ, or Δ to Y). Motor impedances are used in the PINN for training the model circuit element values. The entire parametrization process is able to be performed within several minutes by a common PC.

2 PINN-based High-Frequency Modeling

Figure 2 exhibits the model equivalent circuit per phase. It comprises 18 circuit elements. L_c and L_c' represent the stator leakage inductances at the beginning several turns. C_{g1}, C_{g2}, and C_g' represent the phase-to-ground parasitic capacitances. R_{g1}, R_{g2}, and R_g' represent the equivalent copper skin and proximity-effect resistances. L_s and L_s' denote the stator-winding leakage inductances. R_e and R_e' denote the high-frequency eddy-current losses of the stator core. R_t, L_t, C_t, R_t', L_t', and C_t' denote the stator interturn parasitic effects. Noted that the model 3-phase equivalent circuit can be built with 3 per phase equivalent circuits according to the motor connection (Y or Δ).

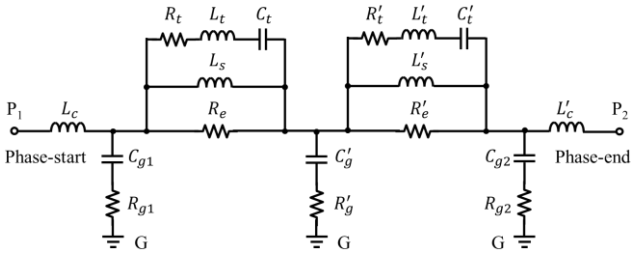

Figure 2. Model equivalent circuit (per phase).

To obtain the circuit element values per phase, 3 motor impedances Z_{P_1G}, Z_{P_2G}, and $Z_{P_1P_2}$ are used in the PINN. Z_{P_1G}, Z_{P_2G}, and $Z_{P_1P_2}$ are the phase-start to ground, phase-end to ground, and phase-start to phase-end impedances, respectively. As shown in Figure 3, the PINN has 6

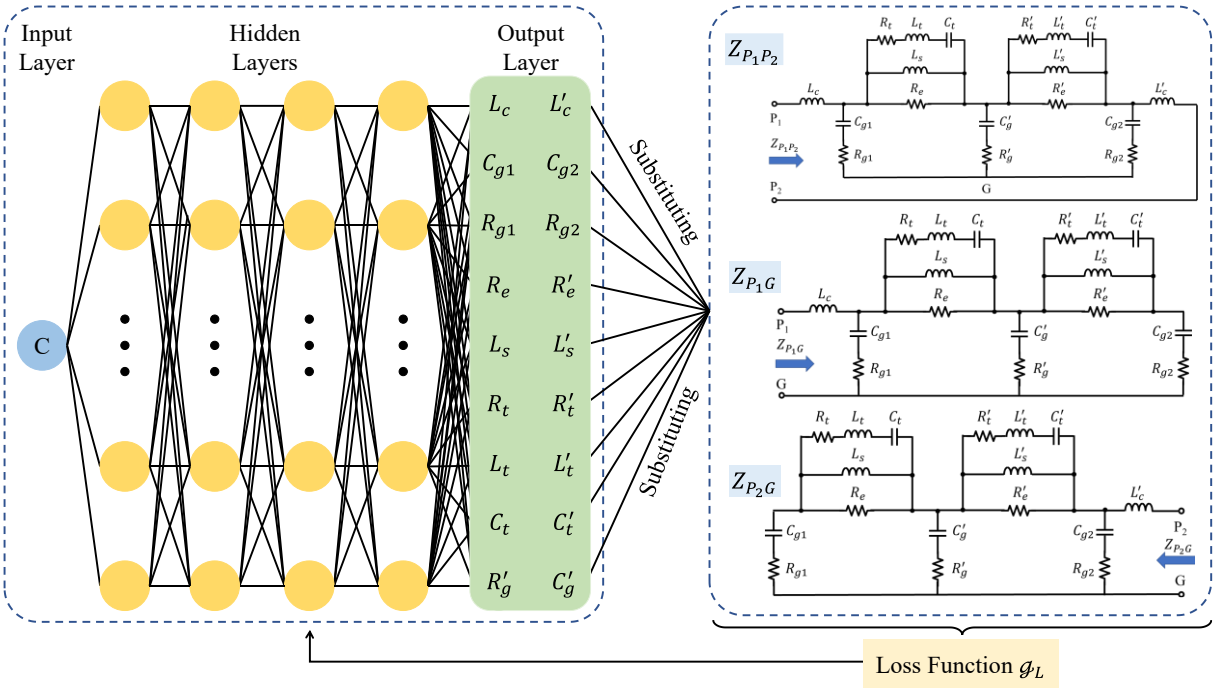

Figure 3. PINN for model circuit elements extraction.

layers: 1 input layer, 4 hidden layers, and 1 output layer. A random constant C is used as the input. The estimated model circuit element values are the output. For the 4 hidden layers, their number of neurons are 50, 200, 200, and 50. The loss function (g_L) is defined by:

$$g_L = \frac{g_L(|Z|) + g_L(\angle Z)}{2} \quad (1)$$

$$g_L(|Z|) = \frac{g_L(|Z_{P_1P_2}|) + g_L(|Z_{P_1G}|) + g_L(|Z_{P_2G}|)}{3} \quad (2)$$

$$g_L(\angle Z) = \frac{g_L(\angle Z_{P_1P_2}) + g_L(\angle Z_{P_1G}) + g_L(\angle Z_{P_2G})}{3} \quad (3)$$

$$g_L(|Z_{P_1P_2}|) = \frac{1}{n}\sum_{i=1}^{n} \log_{10}\left[\cosh\left(1 - \frac{|\tilde{Z}_{P_1P_2}|}{|Z_{P_1P_2}|}\right)\right] \quad (4)$$

$$g_L(|Z_{P_1G}|) = \frac{1}{n}\sum_{i=1}^{n} \log_{10}\left[\cosh\left(1 - \frac{|\tilde{Z}_{P_1G}|}{|Z_{P_1G}|}\right)\right] \quad (5)$$

$$g_L(|Z_{P_2G}|) = \frac{1}{n}\sum_{i=1}^{n} \log_{10}\left[\cosh\left(1 - \frac{|\tilde{Z}_{P_2G}|}{|Z_{P_2G}|}\right)\right] \quad (6)$$

$$g_L(\angle Z_{P_1P_2}) = \frac{1}{n}\sum_{i=1}^{n} \log_{10}\left[\cosh\left(1 - \frac{\angle\tilde{Z}_{P_1P_2} + \Delta}{\angle Z_{P_1P_2} + \Delta}\right)\right] \quad (7)$$

$$g_L(\angle Z_{P_1G}) = \frac{1}{n}\sum_{i=1}^{n} \log_{10}\left[\cosh\left(1 - \frac{\angle\tilde{Z}_{P_1G} + \Delta}{\angle Z_{P_1G} + \Delta}\right)\right] \quad (8)$$

$$g_L(\angle Z_{P_2G}) = \frac{1}{n}\sum_{i=1}^{n} \log_{10}\left[\cosh\left(1 - \frac{\angle\tilde{Z}_{P_2G} + \Delta}{\angle Z_{P_2G} + \Delta}\right)\right] \quad (9)$$

where $Z_{P_1P_2}$, Z_{P_1G}, and Z_{P_2G} can be measured with an impedance analyzer; $\tilde{Z}_{P_1P_2}$, $\tilde{Z}_{P_1G}$, and $\tilde{Z}_{P_2G}$ represent the estimated values using the PINN; n denotes the number of points over an interested frequency range. By minimizing g_L, the model circuit element values in each phase can be obtained finally.

3 Case Study

A 7.5 hp induction motor (AEEBKB067R50FM) was chosen for experimental validation. An impedance analyzer (Keysight E4990A) was used to measure $Z_{P_1P_2}$, Z_{P_1G}, and Z_{P_2G} from 1 kHz to 30 MHz for all 3 phases. n was set to 1186. A common PC (2.40-GHz 8-core) was selected as the platform of parameterization. For the parameterization's stop condition, it was set that the mean absolute relative error (MARE) of $|Z_{P_1P_2}|$, $|Z_{P_1G}|$, and $|Z_{P_2G}|$ are decreased to 1.5 dB, and the mean absolute error (MAE) of $\angle Z_{P_1P_2}$, $\angle Z_{P_1P_2}$, and $\angle Z_{P_1P_2}$ are decreased to 9.0°. The time of the entire parameterization was around 5 minutes. Table 1 gives the estimated motor circuit element values for all 3 phases.

In order to validate the constructed model's accuracy to predict its DM and CM impedances under Y and Δ connections, the measured impedances using an impedance analyzer are used as references. Based on the circuit element values in Table 1, Figure 4 shows simulated Z_{CM-Y} and Z_{DM-Y}. Similarly, Figure 5 shows simulated $Z_{CM-\Delta}$ and $Z_{DM-\Delta}$. The measured impedances are also listed in Figures 4 and 5 for ease of comparison.

Table 1. Estimated motor circuit element values

Element	Phase A	Phase B	Phase C
L_c	0.28 µH	0.25 µH	0.30 µH
C_{g1}	426 pF	568 pF	691 pF
R_{g1}	6.52 Ω	6.77 Ω	7.84 Ω
R_e	1.82 kΩ	1.86 kΩ	8.71 kΩ
L_s	20.5 mH	18.1 mH	15.3 mH
R_t	43.2 kΩ	42.6 kΩ	2.93 kΩ
L_t	10.3 mH	41.6 mH	0.94 mH
C_t	2.75 pF	2.55 pF	3.98 pF
R'_g	50.8 Ω	58.4 Ω	201 Ω
L'_c	0.31 µH	0.33 µH	0.20 µH
C_{g2}	631 pF	631 pF	601 pF
R_{g2}	5.38 Ω	5.98 Ω	12.5 Ω
R'_e	1.80 kΩ	1.98 kΩ	14.2 kΩ
L'_s	16.0 mH	15.5 mH	12.4 mH
R'_t	37.8 kΩ	42.8 kΩ	2.30 kΩ
L'_t	11.1 mH	40.7 mH	0.34 mH
C'_t	2.76 pF	2.54 pF	3.29 pF

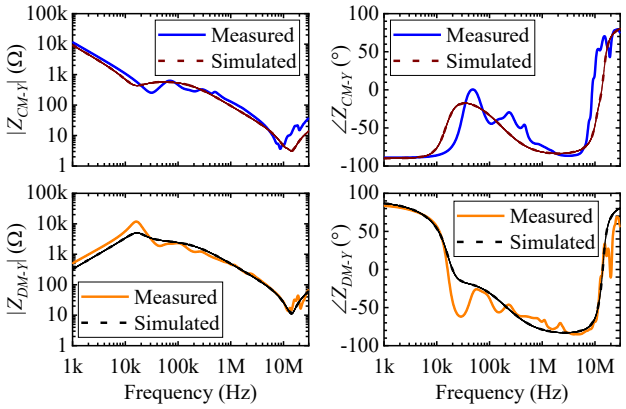

Figure 4. Simulated and measured Z_{CM-Y} and Z_{DM-Y}.

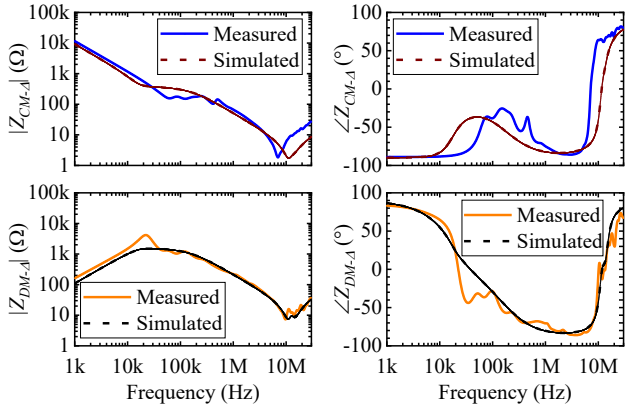

Figure 5. Simulated and measured $Z_{CM-\Delta}$ and $Z_{DM-\Delta}$.

As can be seen, the simulated Z_{CM-Y}, Z_{DM-Y}, $Z_{CM-\Delta}$, and $Z_{DM-\Delta}$ have rather small deviations with the measured Z_{CM-Y}, Z_{DM-Y}, $Z_{CM-\Delta}$, and $Z_{DM-\Delta}$ in both magnitude and phase over the entire frequency range of interest. Thus, the high precision of the proposed method for motor CM and DM impedances prediction is validated. Besides, it also demonstrates its good generality for both Y and Δ connected induction motors.

4 Conclusions

This paper introduces a PINN-based method for induction motor high-frequency behavioral modeling. The presented model owes high precision, good generality, and easy parameterization. The case study has validated the capability of this method and its high precision to estimate the motor wideband (i.e., 1 kHz to 30 MHz) DM and CM impedances under Y and Δ connections. This promises a precise evaluation of the overvoltage as well as the conducted EMI in motor drive systems.

References

[1] G. Skibinski, R. Kerkman, D. Leggate, J. Pankau, and D. Schlegel, "Reflected wave modeling techniques for PWM AC motor drives," in *Proc. Appl. Power Electron. Conf. (APEC)*, Anaheim, CA, USA, 1998, pp. 1021-1029, doi: 10.1109/APEC.1998.654023.

[2] G. Grandi, D. Casadei, and U. Reggiani, "Common- and differential-mode HF current components in AC motors supplied by voltage source inverters," *IEEE Trans. Power Electron.*, vol. 19, no. 1, pp. 16-24, Jan. 2004, doi: 10.1109/TPEL.2003.820564.

[3] L. Wang, C. N.-M. Ho, F. Canales, and J. Jatskevich, "High-frequency modeling of the long-cable-fed induction motor drive system using TLM approach for predicting overvoltage transients," *IEEE Trans. Power Electron.*, vol. 25, no. 10, pp. 2653-2664, Oct. 2010, doi: 10.1109/TPEL.2010.2047027.

[4] Y. Ryu, M. Yea, J. Kim, and K. J. Han, "Stator impedance modeling platform for the electromagnetic compatibility aware design of 3.7-to 7.5-kW squirrel-cage induction motors," *IEEE Trans. Ind. Electron.*, vol. 68, no. 11, pp. 11255-11265, Nov. 2021, doi: 10.1109/TIE.2020.3032925.

[5] A. F. Moreira *et al.*, "High-frequency modeling for cable and induction motor overvoltage studies in long cable drives," *IEEE Trans. Ind. Appl.*, vol. 38, no. 5, pp. 1297-1306, Sep./Oct. 2002, doi: 10.1109/TIA.2002.802920.

[6] J. Sun and L. Xing, "Parameterization of three-phase electric machine models for EMI simulation," *IEEE Trans. Power Electron.*, vol. 29, no. 1, pp. 36-41, Jan. 2014, doi: 10.1109/TPEL.2013.2264750.

[7] M. S. Toulabi *et al.*, "A universal high-frequency induction machine model and characterization method for arbitrary stator winding connections," *IEEE Trans. Energy Convers.*, vol. 34, no. 3, pp. 1164-1177, Sep. 2019, doi: 10.1109/TEC.2019.2891349.